

УДК 538.9

EFFECT OF PRESSURE ON ELECTRONIC AND OPTICAL PROPERTIES OF MAGNESIUM SILICIDE AND GERMANIDE¹

V. L. SHAPOSHNIKOV^a, A. V. KRIVOSHEEVA^a, V. E. BORISENKO^a

^aBelarusian State University of Informatics and Radioelectronics,
P. Brovki street, 6, 220013, Minsk, Republic of Belarus
Corresponding author: victor.shaposhnikov@gmail.com

A detailed theoretical study of electronic and optical properties of magnesium silicide Mg₂Si and germanide Mg₂Ge under hydrostatic and uniaxial pressure has been performed by means of linearized augmented plane wave method. It has been found that the direct gap at the Γ -point increases linearly with the rise of the pressure, while the indirect one decreases becoming zero under the hydrostatic pressure of about 10 GPa. The decrease of the static dielectric constant with the rise of the pressure reflects the changes in the direct gap. Quite different results were observed for uniaxial deformation of the lattice. Either compression or tension of the lattice strongly decreases the indirect band gap. The direct gap depends linearly on the both types of deformations, but dependencies have different slopes.

Key words: magnesium silicide; magnesium germanide; hydrostatic pressure; uniaxial deformation; isotropic deformation.

¹Статья публикуется в авторской редакции.

Образец цитирования:

Шапошников В. Л., Кривошеева А. В., Борисенко В. Е. Влияние давления на электронные и оптические свойства силицида и германида магния // Журн. Белорус. гос. ун-та. Физика. 2017. № 1. С. 73–81.

For citation:

Shaposhnikov V. L., Krivosheeva A. V., Borisenko V. E. Effect of pressure on electronic and optical properties of magnesium silicide and germanide. *J. Belarus. State Univ. Phys.* 2017. No. 1. P. 73–81 (in Engl.).

Авторы:

Виктор Львович Шапошников – кандидат физико-математических наук; старший научный сотрудник кафедры микро- и нанoeлектроники факультета радиотехники и электроники.

Анна Владимировна Кривошеева – кандидат физико-математических наук; старший научный сотрудник кафедры микро- и нанoeлектроники факультета радиотехники и электроники.

Виктор Евгеньевич Борисенко – доктор физико-математических наук, профессор; заведующий кафедрой микро- и нанoeлектроники факультета радиотехники и электроники.

Authors:

Victor Shaposhnikov, PhD (physics and mathematics); senior researcher at the department of micro- and nanoelectronics, faculty of radioengineering and electronics.

victor.shaposhnikov@gmail.com

Anna Krivosheeva, PhD (physics and mathematics); senior researcher at the department of micro- and nanoelectronics, faculty of radioengineering and electronics.

anna@nano.bsuir.edu.by

Victor Borisenko, doctor of science (physics and mathematics), full professor; head of the department of micro- and nanoelectronics, faculty of radioengineering and electronics.

borisenko@bsuir.by

ВЛИЯНИЕ ДАВЛЕНИЯ НА ЭЛЕКТРОННЫЕ И ОПТИЧЕСКИЕ СВОЙСТВА СИЛИЦИДА И ГЕРМАНИДА МАГНИЯ

В. Л. ШАПОШНИКОВ¹⁾, А. В. КРИВОШЕЕВА¹⁾, В. Е. БОРИСЕНКО¹⁾

¹⁾Белорусский государственный университет информатики и радиоэлектроники,
ул. П. Бровки, 6, 220013, г. Минск, Республика Беларусь

Представлены результаты детальных теоретических исследований электронных и оптических свойств силицида магния Mg_2Si и германида магния Mg_2Ge , подвергнутых воздействию гидростатического и одноосного давления, выполненных с помощью метода линеаризованных присоединенных плоских волн. Определено, что прямой переход в Γ -точке линейно возрастает с увеличением давления, в то время как непрямой переход уменьшается до нуля при гидростатическом давлении 10 ГПа. Уменьшение статической диэлектрической проницаемости с повышением давления отражает изменения в прямом переходе. При одноосной деформации как сжатие, так и растяжение решетки значительно уменьшают непрямой переход. Зависимости изменения прямого перехода при двух типах деформации имеют линейный характер, но разный угол наклона.

Ключевые слова: силицид магния; германид магния; гидростатическое давление; одноосная деформация; изотропная деформация.

Introduction

Last years the interest to Mg_2X compounds and also their ternary alloys reappeared as to ecologically clean semiconductors, which consist of non-toxic materials and possess high value of the power factor and thermoelectric figure of merit as compared with GeSi alloys and β -FeSi [1; 2]. Magnesium silicide (Mg_2Si) together with isostructural magnesium germanide (Mg_2Ge) are well known as promising materials for thermoelectric energy conversion applications [3–6] because of large Seebeck coefficient, low electrical resistivity, and low thermal conductivity [7]. Moreover, practical interest to Mg_2Si is explaining by their attractive properties and good compatibility with the conventional silicon technology [8]. The quality of semiconductor devices strongly depends on structural matching between the substrate and the epitaxial film. The lattice mismatch leads to uniaxial and isotropic deformations at the interface, which may influence their fundamental properties and lead to considerable difference from the relaxed materials. A range of physical properties of Mg_2Si and Mg_2Ge depend on its lattice behavior. The high symmetry of the structure implies that external impact like pressure or electric field could lead to appearance of piezoelectric effects or possible degeneration of bands with negative masses [9]. Therefore, it is important to understand the effect of lattice distortion on its electronic and optical properties, while further investigations could lead to enhancement of thermoelectric efficiency [10].

Mg_2Si has been an object of intensive experimental studies since the 1960s [4; 11–17]. However, bulk single crystals, rather than thin films have been examined experimentally owing to difficulties of thin film formation. That is caused by low condensation coefficient and high vapour pressure of magnesium. Even less experimental results can be found for Mg_2Ge . According to the resistivity measurements both compounds were found to be semiconductors with the band gap of 0.80 and 0.69 eV for Mg_2Si and Mg_2Ge , respectively [4; 12; 13]. The low- and room-temperature optical measurements report Mg_2Si to have an indirect gap of 0.60–0.74 eV and a direct one of 0.83–2.17 eV. For Mg_2Ge these values are 0.70 eV and 1.60–1.67 eV for the indirect and direct band gap, respectively [11; 15].

Both semiconductors received a good deal of attention from theoretical point of view [7; 10; 18–29]. According to the calculations performed, Mg_2Si is an indirect-gap semiconductor with the fundamental energy gap of 0.12–1.30 eV. The first direct gap transition is estimated to be 1.55–2.84 eV. Depending on the chosen theoretical approximation the band structure calculations performed for Mg_2Ge give the indirect gap of 0.165–1.60 eV and a direct one of 1.30–2.51 eV [18; 19; 23; 24].

In this paper, we present the dependence of the electronic band gap and optical properties of Mg_2Si and Mg_2Ge on isotropic and anisotropic deformation of their lattices caused by hydrostatic and uniaxial pressure, respectively. It has been obtained by *ab initio* electronic property calculations for pressures up to 12 GPa, that corresponds to 5 % reduction of the lattice parameter.

Computational details

The simulation of the electronic band structure has been carried out by means of the self-consistent full-potential linearized-augmented-plane-wave method in its scalar-relativistic version using WIEN2k package [30].

The generalized gradient approximation (GGA) has been applied in the calculations of the exchange-correlation potential [31; 32]. We used 104 and 220 sampling \mathbf{k} -points in the irreducible Brillouin zone for the self-consistent procedure and for the calculations of the momentum matrix element in the dielectric function, respectively. The real part of the dielectric function has been obtained from the imaginary one through the Kramers – Kronig relation.

Mg_2Si and Mg_2Ge belong to so-called electron-deficient semiconductors [20]. They crystallize in the face-centred-cubic (f. c. c.) CaF_2 -type lattice with $Fm3m$ space group. In the present calculations the lattice parameters of 0.6382 and 0.6435 nm are used for Mg_2Si and Mg_2Ge , respectively. These values are in rather good agreement with experimental ones (0.6338 and 0.6388 nm for Mg_2Si and Mg_2Ge , respectively [4]), with the discrepancy 0.8 %, which occurs due to GGA overestimation of lattice parameters if compare with those obtained from experiment [33; 34]. With the local density approximation (LDA) [35] the larger discrepancies from the experimental values were observed, thus for the compounds considered GGA was chosen as more appropriate.

The hydrostatic pressure has been modelled by reducing the lattice parameter in the range of 0–5 % from the equilibrium value without changing the symmetry of the structure. The corresponding hydrostatic pressure occurred in the system has been calculated as a first volume derivative of the energy. However, when the pressure is applied along one axis ((001) in our case), the change of the symmetry from f. c. c. to tetragonal type structure takes place. The lattice parameters along (100) and (010) directions have been varied in the range of ± 5 % with the step of 1 % from the value of unstressed materials. The lattice parameter along (001) axis

has been calculated using elastic theory by equation: $a_{\perp} = a_{\text{bulk}} \left[1 - \frac{2C_{12}}{C_{11}} \frac{a_{\parallel}}{a_{\text{bulk}} - 1} \right]$, where a_{bulk} is the lattice parameter of unstressed cubic structure; a_{\perp} and a_{\parallel} are the lattice parameters within and perpendicular the plane (001); C_{11} and C_{12} are the elastic constants, taken from experiments [36]. For Mg_2Si they were chosen as 121.0 and 22.0 GPa [37], for Mg_2Ge – 117.9 and 23.0 GPa [38] for C_{11} and C_{12} , respectively.

Results and discussion

The calculated band structures of unstressed Mg_2Si and Mg_2Ge (solid lines) are shown in fig. 1 in comparison with the materials under the hydrostatic pressure (dashed lines) for the case of 5 % reducing of the lattice parameter. In unstressed magnesium compounds the valence band maximum (VBM) locates at the Γ -point, whereas the conduction band minimum (CBM) is at the X-point.

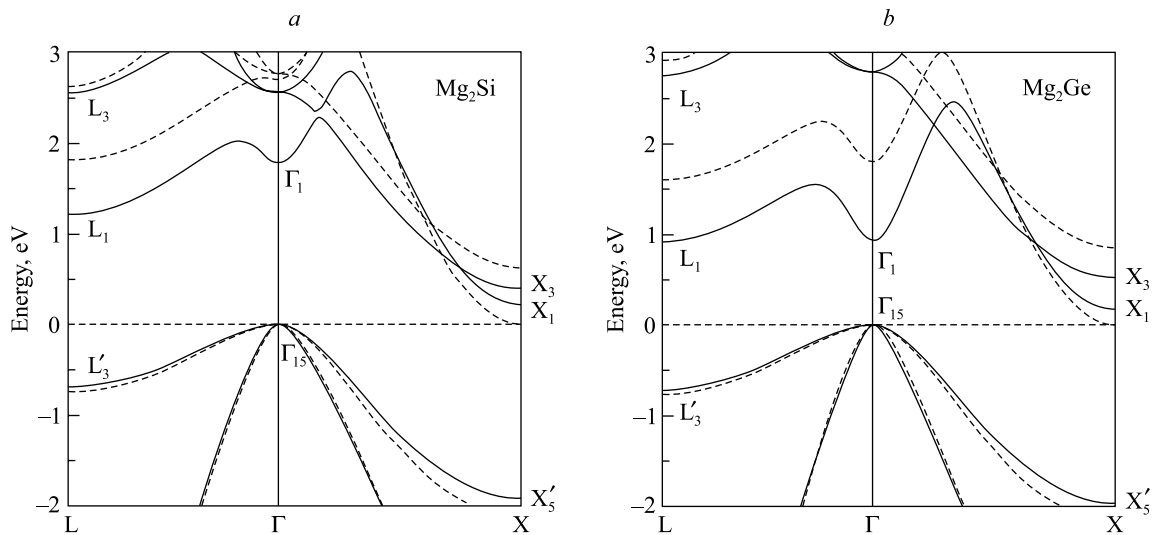


Fig. 1. Electronic band structures of Mg_2Si (a) and Mg_2Ge (b) along the main high-symmetry directions $L-\Gamma-X$. Solid lines correspond to unstressed compounds; dashed ones – to 5 % hydrostatic compression of the lattice. Zero at the energy scale corresponds to the Fermi energy

The first direct transition occurs in the centre of the Brillouin zone. Qualitatively, the band structures obtained are in good agreement with the results of theoretical calculations [18; 19; 21; 23; 24]. Table 1 compares the values of the main interband transitions in Mg_2Si and Mg_2Ge with the theoretical and experimental data.

Table 1

Calculated interband transition energies, eV, in Mg₂Si and Mg₂Ge.
The symbols (*d*) and (*i*) are used for direct or indirect gaps, respectively

Transition	Mg ₂ Si			Mg ₂ Ge		
	Our calculations	Theory ¹	Experiment ²	Our calculations	Theory ¹	Experiment ²
$\Gamma_{15} \rightarrow X_1$	0.22 (<i>i</i>)	0.14–1.30	0.60–0.74	0.17 (<i>i</i>)	0.92–1.60	0.70
$\Gamma_{15} \rightarrow \Gamma_1$	1.79 (<i>d</i>)	1.90–2.84	2.10–2.27	0.91 (<i>d</i>)	1.49–2.51	1.60–1.67
$L'_3 \rightarrow L_1$	1.90	1.97–3.18	–	1.64	1.99–3.20	2.10
$X'_5 \rightarrow X_1$	2.14	2.13–3.10	2.50–2.85	2.14	3.01–3.26	2.57
$X'_5 \rightarrow X_3$	2.32	2.36–3.77	–	2.49	2.84–4.04	–

¹[12; 14; 16];

²[11; 14; 17].

The energy dependencies of the dielectric function for both magnesium compounds are similar in general. The main peaks in the range of 0–5 eV characterize the interband transitions between the two highest valence and the two lowest conduction bands. All the features of the experimental spectra are reproduced by the calculations, in spite of some underestimation of the energy position of the theoretical peaks. The comparison of the static dielectric constant (ϵ_0) (16.2 and 12.9 for Mg₂Si and Mg₂Ge, respectively) with experimental (12.9 and 13.3 [11]; 20.0 and 21.7 [39]) and theoretical (16.2 and 16.4 [24]) data show quite good correlation.

The differences in band spectra between materials with the ideal crystal lattice and under the hydrostatic pressure (fig. 1) can be found in both valence and conduction bands. The behaviour of the top valence and the two lowest conduction band states at some high-symmetry points (HSP) under the hydrostatic pressure is demonstrated in fig. 2. The values are given relatively to 2s(3s)-states of Si (Ge) for Mg₂Si (Mg₂Ge). The energy values were shifted so that the top valence band states at the Γ -point in unstressed material are set to zero. For Mg₂Si the VBM moves down with the increase of the pressure, while it remains practically flat for Mg₂Ge. The opposite situation is observed for the second conduction band, which is flat for Mg₂Si and moves up with an increase of the pressure for Mg₂Ge. The behaviour of the first conduction band for both compounds is similar for the high-symmetry points considered.

The calculated indirect and direct transitions as a function of the hydrostatic pressure are plotted in fig. 3.

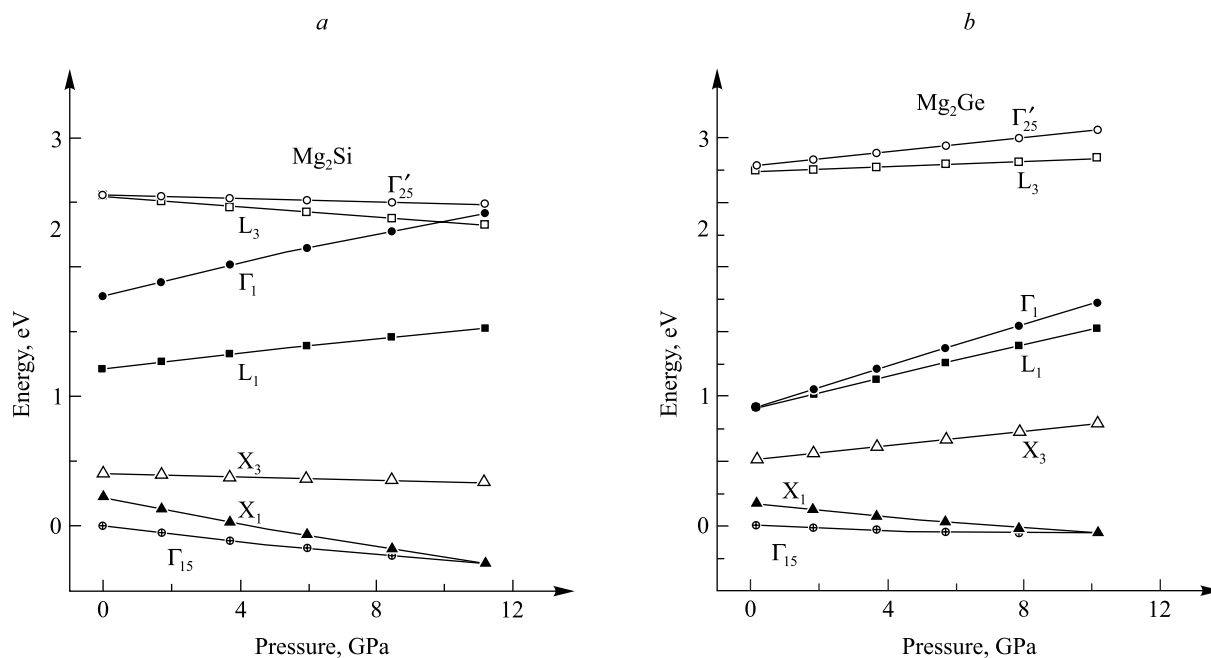


Fig. 2. Energies of the top valence and the two lowest conduction states of Mg₂Si (*a*) and Mg₂Ge (*b*) at some *k*-points as a function of hydrostatic pressure

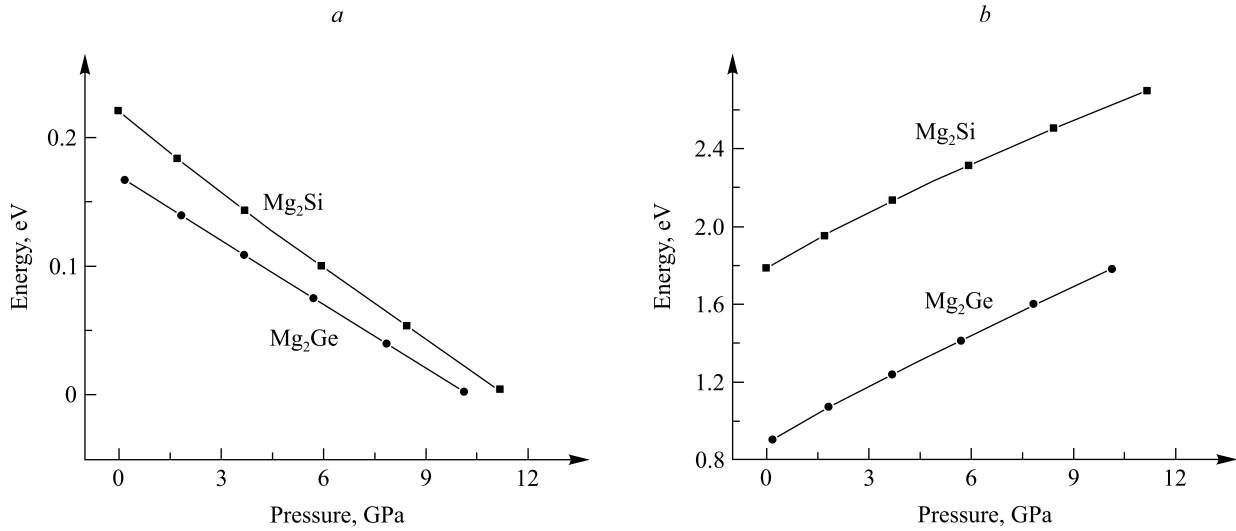


Fig. 3. The behaviour of the main interband transitions in Mg_2Si and Mg_2Ge under the hydrostatic pressure: *a* – for indirect gap, *b* – for direct gap

Both compounds show similar pressure dependence of the transitions. The gap for the direct transition at the Γ -point increases with the rise of the pressure, while the indirect one decreases. The value of conduction band minimum at the Γ -point increases and the value of valence band maximum decreases with the rise of the pressure that leads to the higher values of the first direct transition. In case of the indirect transition between the Γ - and the X-points, both bands move down with the rise of the pressure, so that the band gap becomes smaller. The change rate of the direct and indirect gaps remains practically the same for both magnesium compounds.

The calculated dependencies of the transition energies on the pressure for Mg_2Si and Mg_2Ge can be fitted as $E(P) = E + aP + bP^2$ with the coefficients listed in the table 2.

Table 2

The coefficients describing the dependence of the main transitions on the hydrostatic pressure $E(P) = E + aP + bP^2$

Compound	Transition			
	$\Gamma-\Gamma$		$\Gamma-X$	
	Coefficient			
	<i>a</i> , meV/GPa	<i>b</i> , meV/GPa ²	<i>a</i> , meV/GPa	<i>b</i> , meV/GPa ²
Mg_2Si	99.35	-1.58	-21.34	0.19
Mg_2Ge	98.41	-1.05	-16.79	0.03

It was proved by some additional calculations that the coefficients obtained are also valid for the crystal structure being stretched out. Moreover, it was found that when the Mg_2Ge structure is 6 % stretched of its equilibrium lattice parameter, the direct gap at the Γ -point appears to be lower in energy than the indirect one at the X-point. It means, Mg_2Ge becomes a direct-gap semiconductor, though the physical realization of such experiment seems to be limited. When both magnesium compounds considered are compressed for about 5 % of their lattice parameters they were observed to become gapless semiconductors.

It is interesting to take into account the results of the calculations performed for Si and Ge under the pressure. These compounds also possess f. c. c. crystal structure. There is a good correlation between the pressure behaviour of the electronic and optical properties and the results obtained in [40]. That allows us to assume the general tendency of the gap behaviour under the pressure for magnesium compounds to be correct.

The changes in the band structure of the compounds due to the hydrostatic pressure of the lattice are reflected in the optical properties. The dielectric function spectra of both materials are plotted in fig. 4.

It is observed that all peaks of the dielectric function move towards higher energies when the pressure increases. Since the origins of the peaks in \mathbf{k} -space remains unchanged under the hydrostatic pressure, these shifts of the peaks are the result of the increase of the direct gaps. The interesting feature of the optical properties is the disappearance of the first peak at about 2 eV for Mg_2Ge (which is present in unstressed compound). Figure 5 presents the dependence of the static dielectric function ϵ_0 on the hydrostatic pressure. It is obvious that its values decrease with the pressure due to the rise of the direct gap for both magnesium compounds considered.

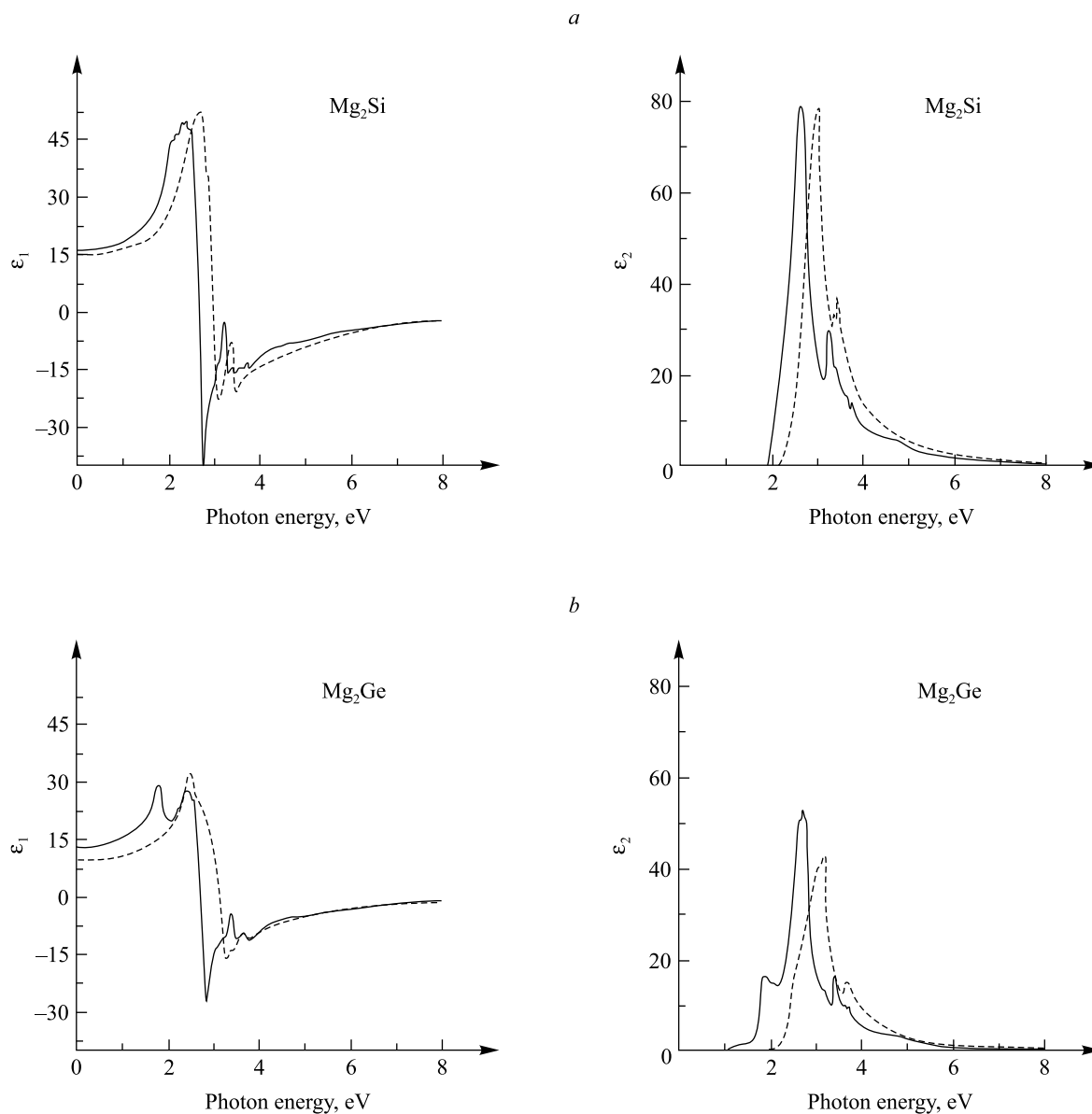


Fig. 4. The real (ϵ_1) and imaginary (ϵ_2) parts of dielectric function of Mg₂Si (a) and Mg₂Ge (b). Solid lines correspond to unstressed compounds; dashed ones – to 5 % hydrostatic compression of the lattice

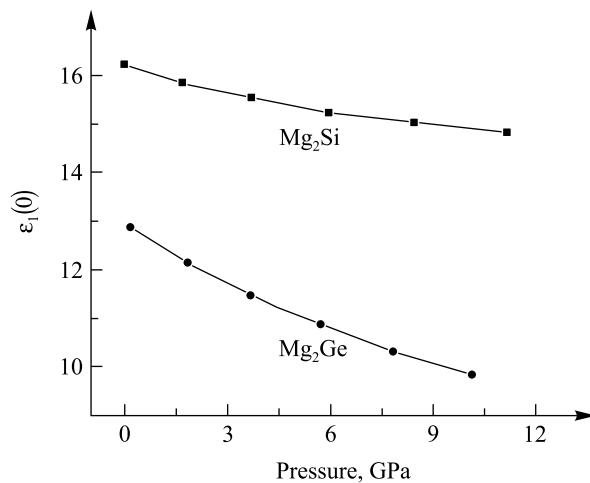


Fig. 5. Static dielectric function ϵ_0 of Mg₂Si and Mg₂Ge as a function of the hydrostatic pressure

The quite different picture was observed for the uniaxial pressure. Figure 6 shows the band structures of Mg_2Si for $\pm 5\%$ variation of the lattice parameter. The similar dependence was observed for Mg_2Ge . For that type of deformation the crystal structure symmetry is changed from f. c. c. to base-centred-tetragonal (b. c. t.) with a quite different Brillouin zone. Thus, the projections of extreme points in f. c. c. may correspond to different points in b. c. t. The VBM is still at the Γ -point, while CBM is located at the X- and Z-points for compression and tension, respectively. The distinctive feature of the uniaxial deformation is the disappearance of the degeneracy at the HSP near the band gap. Moreover, this degeneracy might be reserved at the Γ -point for some bands depending on which uniaxial deformation (compression or tension) is applied.

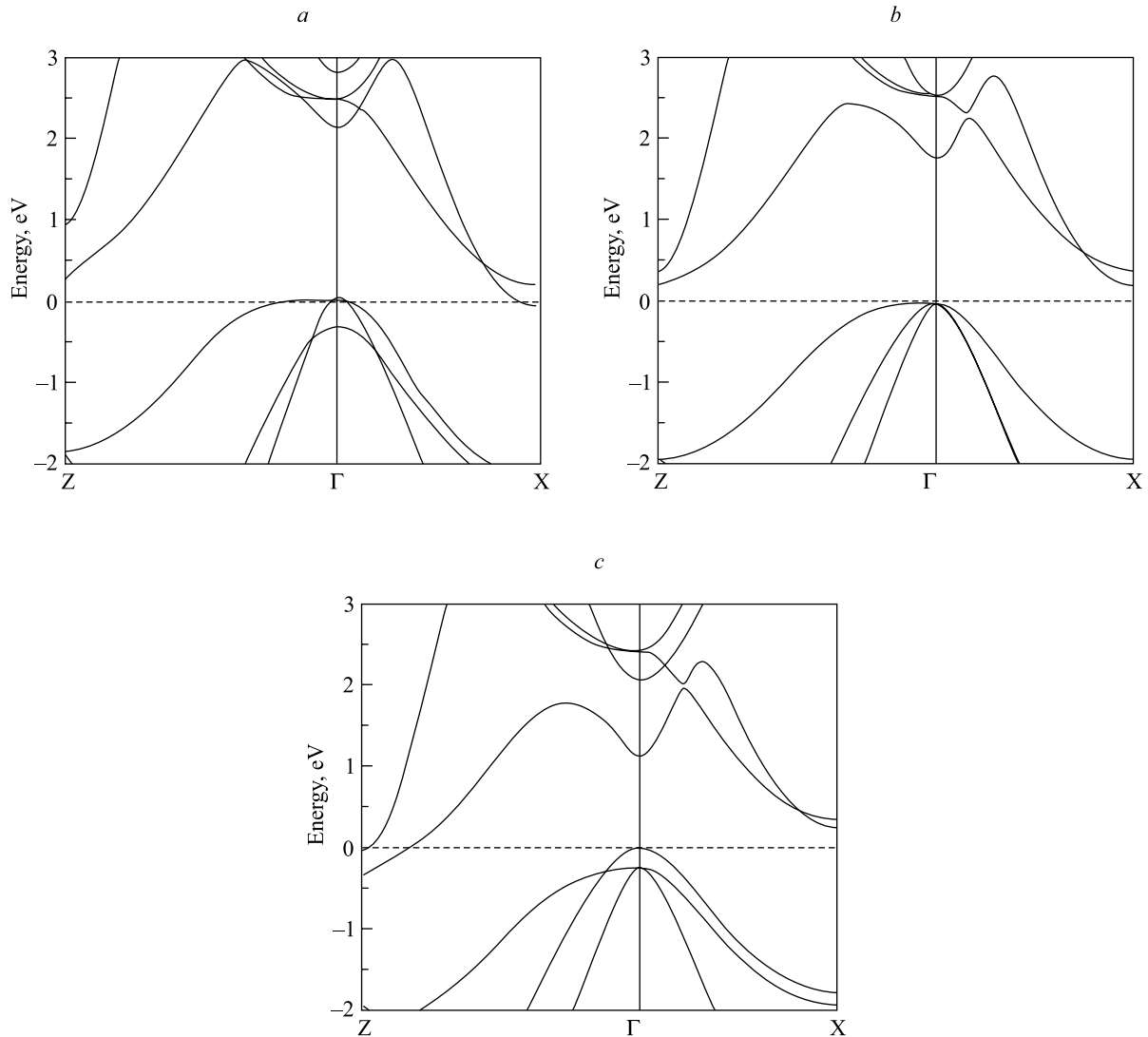


Fig. 6. Electronic band structures of Mg_2Si along the main high-symmetry directions when the 5% uniaxial compression (a) and tension (c) is applied in comparison with unstressed structure (b). Zero at the energy scale corresponds to the Fermi energy

The influence of the uniaxial deformation on the main interband transitions is shown in fig. 7. As it is hard to determine the real pressure occurred in the system, the energy values are plotted versus the change of the lattice parameter. The behaviour of the energy transitions is quite different in comparison with the hydrostatic pressure case, i. e. the rate of the band gap changes is different. The strong decrease of the band gap is observed for uniaxial compression and tension of the lattice with practically similar rates. Thus, both materials become gapless semiconductors at about 3% uniaxial deformation of their structures. That can be explained by the fact, that compression along (100) axis decreases the band gap in this direction more rapidly than the CBM is moved to the high-energy region due to the tension in the plane perpendicular to this axis. The first direct gap at the Γ -point increases under uniaxial compression of the lattice and decreases when the lattice is stretched. The rate of the direct gap increase is somewhat lower than that of the decrease.

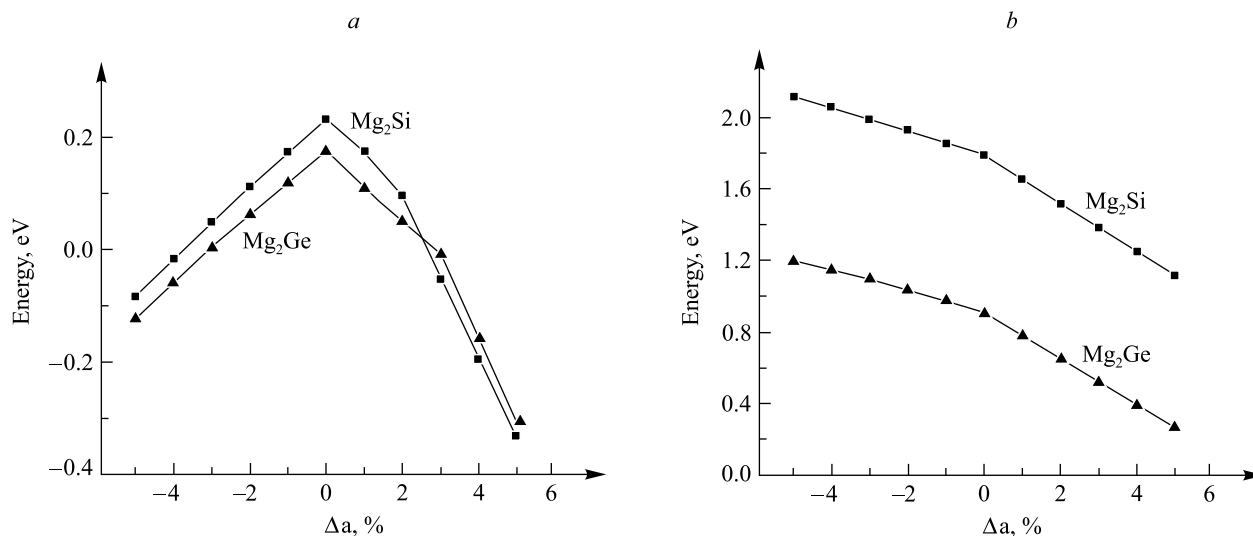


Fig. 7. The behaviour of the main interband transitions in Mg_2Si and Mg_2Ge under the uniaxial deformation: *a* – for indirect gap; *b* – for direct gap

It is well known that band gap values calculated within LDA are underestimated with respect to experimental data. The situation is especially crucial in case of *sp*-bonding semiconductors, the considered compounds belong to. The underestimation depends on the shift of eigenvalues in the energy range analysed via the so-called correlation effects. For the situation considered, the VBM is found to be mainly composed by *p*-electrons of either Si or Ge (depending on the compound). The orbital composition of the first conduction band for both Γ - and X-points is characterized practically completely by *s*-electrons of Si (Ge) with small contribution of other states. As a result, conduction and valence band edges undergo different shifts. However, band gap predictions obtained within DFT approaches for transition metal silicides are often quantitatively correct. For example, in the case of semiconducting iron disilicide we obtained very good agreement between theoretically predicted and experimental values [41] due to almost equal shift of corresponding eigenfunctions at the extreme points, which are mainly composed of *d*-electron states of iron atoms. To solve the problem of the band-gap underestimation one of the simplest ways is the use of so-called «scissors-operator» shift (SOS), which in present work was equal to 0.38 and 0.53 eV for Mg_2Si and Mg_2Ge , respectively, if one takes experimental values from [11] as a true reference. The orbital composition analysis of the extreme points of the band spectra shows it practically not to depend on the pressure applied. That allows us to suppose that the SOS-parameter will be a constant value in the range of the pressure considered. The results obtained here for the magnesium compounds are in good agreement with the experimental data.

Conclusions

The *ab initio* calculations of electronic and optical properties of Mg_2Si and Mg_2Ge performed within the FLAPW method show dramatic influence of the isotropic and anisotropic lattice distortion on resulting spectra. The direct transition in the Γ -point demonstrates a linear increase with the rise of the hydrostatic pressure, while the indirect one decreases and becomes zero at about 5 % compression of the material lattices. When the lattice of Mg_2Ge is 6 % stretched, it becomes a direct gap semiconductor. The static dielectric constant decreases with the rise of the pressure directly reflecting the changes in the direct gap values. In case of uniaxial deformation the indirect band gap strongly decreases at both types of strains applied, making the Mg_2X materials to be gapless at about 3 % strains. The direct gap depends linearly on the both types of deformation but with the different rates.

The authors would like to thank doctors A. N. Kholod, N. N. Dorozhkin and D. B. Migas for helpful discussion of the results obtained.

REFERENCES

1. Galkin N. G., Galkin K. N., Goroshko D. L., et al. Non-doped and doped Mg stannide films on Si(111) substrates: formation, optical, and electrical properties. *Jpn. J. Appl. Phys.* 2015. Vol. 54. 07JC06. DOI: 10.7567/JJAP.54.07JC06.
2. Chuang L., Savvides N., Tan T. T., et al. Thermoelectric properties of Ag-doped Mg_2Ge thin films prepared by magnetron sputtering. *J. Electron. Mater.* 2010. Vol. 39, issue 9. P. 1971–1974. DOI: 10.1007/s11664-009-1052-4.
3. Kajikawa T., Shida K., Shiraishi K., et al. Thermoelectric figure of merit of impurity doped and hot-pressed magnesium silicide elements. *XVII Int. Conf. on Thermoelectrics* : proc. ICT'98 (Nagoya, 24–28 May 1998). Nagoya, 1998. P. 362–369.
4. LaBotz R. J., Mason D. R., O'Kane D. F. The thermoelectric properties of mixed crystals of $Mg_2Ge_xSi_{1-x}$. *J. Electrochem. Soc.* 1963. Vol. 110, No. 2. P. 127–134.
5. Noda Y., Kon H., Furukawa Y., et al. Preparation and thermoelectric properties of $Mg_2Si_{1-x}Ge_x$ ($x = 0.0 \sim 0.4$) solid solution semiconductors. *Mater. Trans.* 1992. Vol. 33, No. 9. P. 845–850.

6. Kaibe H. T., Noda Y., Isoda Y., et al. Temperature dependence of thermal conductivity for $\text{Mg}_x\text{Si}_{1-x}\text{Ge}_x$ solid solution. *XVI Int. Conf. on Thermoelectrics* : proceedings (Piscataway, 26–29 August 1997). Piscataway, 1997. P. 279–282.
7. Tani J.-I., Kido H. Lattice dynamics of Mg_2Si and Mg_2Ge compounds from first-principles calculations. *Comput. Mater. Sci.* 2008. Vol. 42. P. 531–536. DOI: 10.1016/j.commatsci.2007.08.018.
8. Semiconducting Silicides. Ed. by V. E. Borisenko. Berlin, 2000.
9. Kroemer H., Day G. F., Fairman R. D., et al. Preparation and some properties of Mg_2Ge single crystals and of $\text{Mg}_2\text{Ge } p-n$ junctions. *J. Appl. Phys.* 1965. Vol. 36, issue 8. P. 2461–2470. DOI: 10.1063/1.1714512.
10. Bessas D., Simon R. E., Friese K., et al. Lattice dynamics in intermetallic Mg_2Ge and Mg_2Si . *J. Phys. : Condens. Matter.* 2014. Vol. 26, No. 48. Article ID 485401. DOI: 10.1088/0953-8984/26/48/485401.
11. Scouler W. J. Optical properties of Mg_2Si , Mg_2Ge , and Mg_2Sn from 0.6 to 11.0 eV at 77 K. *Phys. Rev.* 1969. Vol. 178, issue 3. P. 1353–1357. DOI: 10.1103/PhysRev.178.1353.
12. Morris R. G., Redin R. D., Danielson G. C. Semiconducting properties of Mg_2Si single crystals. *Phys. Rev.* 1958. Vol. 109, issue 6. P. 1909–1915. DOI: 10.1103/PhysRev.109.1909.
13. Redin R. D., Morris R. G., Danielson G. C. Semiconducting properties of Mg_2Ge single crystals. *Phys. Rev.* 1958. Vol. 109, issue 6. P. 1916–1920. DOI: 10.1103/PhysRev.109.1916.
14. Mahan J. E., Vantomme A., Langouche G., et al. Semiconducting Mg_2Si thin films prepared by molecular-beam epitaxy. *Phys. Rev. B.* 1996. Vol. 54, issue 23. P. 16965–16971. DOI: 10.1103/PhysRevB.54.16965.
15. Vazquez F., Forman R. A., Cardona M. Electroreflectance measurements on Mg_2Si , Mg_2Ge , and Mg_2Sn . *Phys. Rev.* 1968. Vol. 176, issue 3. P. 905–908.
16. Stella A., Lynch D. W. Photoconductivity in Mg_2Si and Mg_2Ge . *J. Phys. Chem. Solids.* 1964. Vol. 25, No. 11. P. 1253–1259. DOI: 10.1016/0022-3697(64)90023-X.
17. Stella A., Brothers A. D., Hopkins R. H., et al. Pressure coefficient of the band gap in Mg_2Si , Mg_2Ge , and Mg_2Sn . *Phys. Stat. Solidi.* 1967. Vol. 23, issue 2. P. 697–702. DOI: 10.1002/pssb.19670230231.
18. Au-Yang M. Y., Cohen M. L. Electronic structure and optical properties of Mg_2Si , Mg_2Ge , and Mg_2Sn . *Phys. Rev.* 1969. Vol. 178, issue 3. P. 1358–1364. DOI: 10.1103/PhysRev.178.1358.
19. Viennois R., Jund P., Colinet C., Tédenac J.-C. Defect and phase stability of solid solutions of Mg_2X with an antiferroite structure: an ab initio study. *J. Solid State Chem.* 2012. Vol. 193. P. 133–136. DOI: 10.1016/j.jssc.2012.04.048.
20. Meloni F., Mooser E., Baldereschi A. Bonding nature of conduction states in electron-deficient semiconductors: Mg_2Si . *Physica B + C.* 1983. Vol. 117/118. P. 72–74. DOI: 10.1016/0378-4363(83)90444-8.
21. Wood D. M., Zunger A. Electronic structure of generic semiconductors: antiferroite silicide and III–V compounds. *Phys. Rev. B.* 1986. Vol. 34, issue 6. P. 4105–4120.
22. Folland N. O. Self-consistent calculations of the energy band structure of Mg_2Si . *Phys. Rev.* 1967. Vol. 158. P. 764–775. DOI: 10.1103/PhysRev.158.764.
23. Lee P. M. Electronic structure of magnesium silicide and magnesium germanide. *Phys. Rev.* 1964. Vol. 135. P. A1110–A1114. DOI: 10.1103/PhysRev.135.A1110.
24. Benhelal O., Chahed A., Laksari S., et al. First-principles calculations of the structural, electronic and optical properties of IIA–IV antiferroite compounds. *Phys. Stat. Solidi (b).* 2005. Vol. 242, issue 10. P. 2022–2032. DOI: 10.1002/pssb.200540063.
25. Bashenov V. K., Mutal A. M., Timofeenko V. V. Valence-band density of states for Mg_2Si from pseudopotential calculation. *Phys. Stat. Solidi (b).* 1978. Vol. 87, issue 2. P. K77–K79. DOI: 10.1002/pssb.2220870247.
26. Arnaud B., Alouani M. All-electron projector-augmented-wave GW approximation: application to the electronic properties of semiconductors. *Phys. Rev. B.* 2000. Vol. 62, issue 7. P. 4464–4476. DOI: 10.1103/PhysRevB.62.4464.
27. Arnaud B., Alouani M. Electron-hole excitations in Mg_2Si and Mg_2Ge compounds. *Phys. Rev. B.* 2001. Vol. 64, issue 3. Article ID 033202. DOI: 10.1103/PhysRevB.64.033202.
28. Chen Q., Xie Q., Zhao F.-J., et al. First-principles calculations of electronic structure and optical properties of strained Mg_2Si . *Chin. Sci. Bull.* 2010. Vol. 55, issue 21. P. 2236–2242. DOI: 10.1007/s11434-010-3280-7.
29. Krivosheeva A. V., Kholod A. N., Shaposhnikov V. L., et al. Band structure of Mg_2Si and Mg_2Ge semiconducting compounds with a strained crystal lattice. *Semiconductors.* 2002. Vol. 36, issue 5. P. 496–500. DOI: 10.1134/1.1478538.
30. Blaha P., Schwarz K., Madsen G. K. H., et al. WIEN2k, An Augmented Plane Wave + Local Orbitals Program For Calculating Crystal Properties. Wien, 2001.
31. Perdew J. P., Chevary J. A., Vosko S. H., et al. Atoms, molecules, solids, and surfaces: Applications of the generalized gradient approximation for exchange and correlation. *Phys. Rev. B.* 1992. Vol. 46, issue 11. P. 6671–6687. DOI: 10.1103/PhysRevB.46.6671.
32. Perdew J. P., Burke K., Ernzerhof M. Generalized gradient approximation made simple. *Phys. Rev. Lett.* 1996. Vol. 77, issue 18. P. 3865–3868. DOI: 10.1103/PhysRevLett.77.3865.
33. Lee I.-H., Martin R. M. Applications of the generalized-gradient approximation to atoms, clusters, and solids. *Phys. Rev. B.* 1997. Vol. 56, issue 12. P. 7197–7205. DOI: 10.1103/PhysRevB.56.7197.
34. Dal Corso A., Pasquarello A., Baldereschi A., et al. Generalized-gradient approximations to density-functional theory: A comparative study for atoms and solids. *Phys. Rev. B.* 1996. Vol. 53, issue 3. P. 1180–1185. DOI: 10.1103/PhysRevB.53.1180.
35. Perdew J. P., Wang Y. Accurate and simple analytic representation of the electron-gas correlation energy. *Phys. Rev. B.* 1992. Vol. 45, issue 23. P. 13244–13249. DOI: 10.1103/PhysRevB.45.13244.
36. Jain S. C., Willis J. R., Bullough R. A review of theoretical and experimental work on the structure of $\text{Ge}_x\text{Si}_{1-x}$ strained layers and superlattices, with extensive bibliography. *Adv. Phys.* 1990. Vol. 39. P. 127–190. DOI: 10.1080/00018739000101491.
37. Whitten W. B., Chung P. L., Danielson G. C. Elastic constants and lattice vibration frequencies of Mg_2Si . *J. Phys. Chem. Solids.* 1965. Vol. 26, issue 1. P. 49–56. DOI: 10.1016/0022-3697(65)90071-5.
38. Chung P. L., Whitten W. B., Danielson G. C. Lattice dynamics of Mg_2Ge . *J. Phys. Chem. Solids.* 1965. Vol. 26, issue 12. P. 1753–1760. DOI: 10.1016/0022-3697(65)90206-4.
39. Madelung O. *Semiconductors: Data handbook*. 3rd ed. Berlin, 2004. P. 465–470.
40. Alouani M., Wills J. M. Calculated optical properties of Si, Ge, and GaAs under hydrostatic pressure. *Phys. Rev. B.* 1996. Vol. 54, issue 4. P. 2480–2490. DOI: 10.1103/PhysRevB.54.2480.
41. Filonov A. B., Migas D. B., Shaposhnikov V. L., et al. Electronic and related properties of crystalline semiconducting iron disilicide. *J. Appl. Phys.* 1996. Vol. 79, issue 10. P. 7708–7712. DOI: 10.1063/1.362436.

Received by editorial board 06.07.2016.